An Evaluation of the Basis and Consequences of a Stay-Green Mutation in the *navel negra* Citrus Mutant Using Transcriptomic and Proteomic Profiling and Metabolite Analysis[1][W]

Enriqueta Alós[2], María Roca, Domingo José Iglesias, Maria Isabel Mínguez-Mosquera, Cynthia Maria Borges Damasceno, Theodore William Thannhauser, Jocelyn Kenneth Campbell Rose, Manuel Talón*, and Manuel Cercós

Instituto Valenciano de Investigaciones Agrarias, Centro de Genómica, 46113 Moncada, Valencia, Spain (E.A., D.J.I., M.T., M.C.); Chemistry and Biochemistry Pigments Group, Food Biotechnology Department, Instituto de la Grasa, Consejo Superior de Investigaciones Científicas, 41012 Sevilla, Spain (M.R., M.I.M.-M.); Department of Plant Biology, Cornell University, Ithaca, New York 14853 (C.M.B.D., J.K.C.R.); and U.S. Department of Agriculture Plant, Soil, and Nutrition Laboratory, Cornell University, Ithaca, New York 14853 (T.W.T.)

A *Citrus sinensis* spontaneous mutant, *navel negra* (*nan*), produces fruit with an abnormal brown-colored flavedo during ripening. Analysis of pigment composition in the wild-type and *nan* flavedo suggested that typical ripening-related chlorophyll (Chl) degradation, but not carotenoid biosynthesis, was impaired in the mutant, identifying *nan* as a type C stay-green mutant. *nan* exhibited normal expression of Chl biosynthetic and catabolic genes and chlorophyllase activity but no accumulation of dephytylated Chl compounds during ripening, suggesting that the mutation is not related to a lesion in any of the principal enzymatic steps in Chl catabolism. Transcript profiling using a citrus microarray indicated that a citrus ortholog of a number of *SGR* (for *STAY-GREEN*) genes was expressed at substantially lower levels in *nan*, both prior to and during ripening. However, the pattern of catabolite accumulation and *SGR* sequence analysis suggested that the *nan* mutation is distinct from those in previously described stay-green mutants and is associated with an upstream regulatory step, rather than directly influencing a specific component of Chl catabolism. Transcriptomic and comparative proteomic profiling further indicated that the *nan* mutation resulted in the suppressed expression of numerous photosynthesis-related genes and in the induction of genes that are associated with oxidative stress. These data, along with metabolite analyses, suggest that *nan* fruit employ a number of molecular mechanisms to compensate for the elevated Chl levels and associated photooxidative stress.

Chlorophyll (Chl) degradation is central to the degreening process that is commonly observed in senescing leaves and the ripening of many fruit, and it has been estimated that approximately 1.2 billion tons of Chl are degraded annually (Hendry et al., 1987). However, despite its importance, the basic steps of the Chl catabolic pathway have only recently been elucidated and a few of the associated genes identified (Hörtensteiner, 2006). The degradation of Chl to a colorless fluorescent intermediate (primary fluorescent Chl catabolite [pFCC]) involves four basic steps, which are apparently common to all plants (Fig. 1): chlorophyllase (CLH) dephytylates Chl *a*, producing chlorophyllide *a*; an unknown metal-chelating substance removes magnesium and produces pheophorbide *a*; and finally, pheophorbide *a* oxygenase (PaO) and red Chl catabolite reductase (RCCR) convert pheophorbide *a* to red Chl catabolite (RCC) and then to pFCCs. The conversion of pheophorbide *a* to RCC has been proposed as the key regulatory step of this pathway, since there is evidence indicating that PaO is the only enzyme of this pathway that is induced during senescence (Thomas et al., 2002), in the form of increased transcript abundance (for review, see Hörtensteiner, 2006). The subsequent reactions are species specific and involve multiple structural modifications of the pFCCs, before they are converted into

[1] This work was supported by the Spanish Ministerio de Ciencia y Tecnología (grant nos. AGL2003–08502–C04–01 and GEN2001–4885–C05–03) and the Instituto Nacional de Investigaciones Agrarias (grant nos. RTA03–106, RTA04–013, and RTA05–247). E.A. was the recipient of an Instituto Nacional de Investigación y Tecnología Agraria y Alimentaria (INIA) predoctoral fellowship, and D.J.I. and M.C. were the recipients of INIA-Comunidades Autónomas contracts. J.K.C.R. was supported by the National Science Foundation's Plant Genome Program (award no. DBI 0606595).

[2] Present address: Department of Cell and Developmental Biology, John Innes Centre, Norwich Research Park, Norwich NR4 7UH, UK.

* Corresponding author; e-mail talon_man@gva.es.

The author responsible for distribution of materials integral to the findings presented in this article in accordance with the policy described in the Instructions for Authors (www.plantphysiol.org) is: Manuel Talón (talon_man@gva.es).

[W] The online version of this article contains Web-only data.
www.plantphysiol.org/cgi/doi/10.1104/pp.108.119917

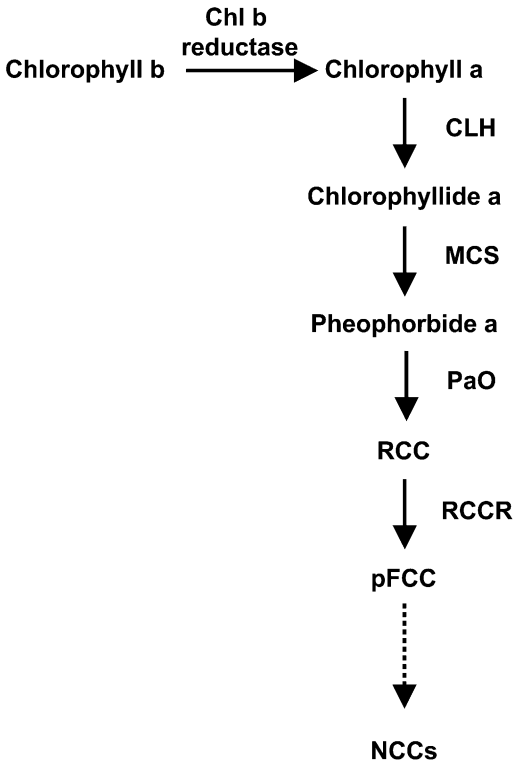

Figure 1. Scheme of the Chl degradative pathway in higher plants. MCS, Metal-chelating substance; NCCs, nonfluorescent chlorophyll catabolites.

nonfluorescent Chl catabolites and are finally stored in the vacuole (Hörtensteiner, 2006). Despite excellent progress in characterizing the primary catabolic events, remarkably little is yet known about the factors that regulate the overall rate and extent of Chl breakdown (Hörtensteiner, 2006).

In this regard, important insights are likely to be provided through the identification and characterization of various "stay-green" mutants that exhibit unusual Chl retention during leaf senescence or fruit ripening (Thomas and Howarth, 2000). Those identified to date span a broad taxonomic range, including members of the Gramineae (durum wheat [*Triticum durum*; Spano et al., 2003]; *Festuca pratensis* [Thomas, 1987]; rice [*Oryza sativa*; Cha et al., 2002; Jiang et al., 2007; Kusaba et al., 2007; Park et al., 2007]), Arabidopsis (*Arabidopsis thaliana*; Woo et al., 2001; Oh et al., 2003, 2004; Ren et al., 2007), and the Leguminosae (soybean [*Glycine max*; Guiamét and Giannibelli, 1994, 1996; Luquez and Guiamét, 2002]; *Phaseolus vulgaris* [Ronning et al., 1991; Bachmann et al., 1994]; pea [*Pisum sativum*; Armstead et al., 2007; Sato et al., 2007]). A stay-green mutant phenotype has also been reported in tomato (*Solanum lycopersicum*) fruits (the *green flesh* mutant; Cheung et al., 1993; Akhtar et al., 1999) and pepper (*Capsicum annuum*; mutant *chlorophyll retainer*; Efrati et al., 2005; Roca and Mínguez-Mosquera, 2006). The molecular bases of the stay-green phenotype were first characterized in a *F. pratensis* mutant line showing accumulation of both Chl *a* and the dephytylated Chl catabolites chlorophyllide *a* and pheophorbide *a* (Thomas et al., 2002). After genetic and biochemical analyses, it was concluded that the mutant was affected in either the *PaO* gene or a specific regulator of this gene. Although biochemical lesions in PaO have been reported for several stay-green mutants (Hörtensteiner, 2006), other types of mutations can also result in stay-green phenotypes, such as Chl *b* reductase in the rice *nyc1* mutant (Kusaba et al., 2007) and genes involved in light-harvesting complex protein II (LHCPII) proteolysis in the *ore9* (Woo et al., 2001) and *ore10* (Oh et al., 2003, 2004) Arabidopsis stay-green mutants. In addition, it has been shown that RNA interference-mediated knockdown of a soybean senescence-associated receptor-like kinase confers a stay-green phenotype (Li et al., 2006).

A clearer understanding of the genetic basis of the control of Chl degradation has only recently resulted from cloning of *STAY-GREEN* (*SGR*) genes from a *Lolium/Festuca* introgression (Armstead et al., 2006), rice (Jiang et al., 2007; Park et al., 2007), pea (Sato et al., 2007), and tomato and pepper (Barry et al., 2008). Although the biochemical function of SGR proteins is not known, they contain a predicted chloroplast transit peptide, and at least one SGR has been shown to bind LHCPII in vivo (Park et al., 2007). Transcript analyses further indicate that *SGR* gene expression is closely associated with leaf senescence (Armstead et al., 2006; Hörtensteiner, 2006; Sato et al., 2007), and transgenic Arabidopsis plants, in which both *SGR1* and *SGR2* genes are suppressed, show a stay-green phenotype, as has been observed in rice (Park et al., 2007). Thus, while *SGR* genes appear to play an important role in one of the early steps of Chl catabolism, much remains to be learned about their mechanism of action. In addition, several transgenic plant lines have been reported that show stay-green phenotypes, such as those induced by altered hormone status, including increased amounts of cytokinins (Smart et al., 1991; Gan and Amasino, 1995) or decreased ethylene production (John et al., 1995). Clearly, numerous factors remain to be discovered that are directly or indirectly important in regulating Chl breakdown, and it is likely that some of these will be identified through characterizing additional stay-green mutations.

This article describes a spontaneous stay-green mutant, *navel negra* (*nan*), from *Citrus sinensis* 'Washington Navel' whose fruit fail to degreen during ripening, although the synthesis of carotenoids is not disrupted. The color change in citrus fruit is particularly evident in the flavedo, the outer colored exocarp of the citrus fruit peel (Davies and Albrigo, 1994), and involves the differentiation of chloroplasts to chromoplasts (Iglesias et al., 2001; Rodrigo et al., 2004) and the biosynthesis of carotenoids. While several studies have described aspects of the latter in citrus fruits (Kato et al., 2004; Rodrigo et al., 2004; Alós et al., 2006), relatively little has been reported about citrus Chl biochemistry, although it has been shown that *CHL*, which is constitutively

expressed during natural fruit development (Jacob-Wilk et al., 1999), is the rate-limiting step of Chl degradation in citrus peel (Harpaz-Saad et al., 2007) and that *PaO* and geranylgeranyl reductase (*CHL P*) gene expression correlates with Chl degradation (Alós et al., 2006). We present here an analysis of the Chl metabolite profile and gene expression pattern in *nan*, which is distinct from previously reported stay-green mutants, that suggests that the mutation is likely associated with an upstream regulatory event rather than with a lesion in a specific step in Chl catabolism. We also describe the use of a citrus microarray and two-dimensional difference gel electrophoresis (2D-DIGE) analysis to contrast the transcriptome and proteome, respectively, of the *nan* flavedo with that of wild-type orange at preripe and ripe stages in order to gain insights into the consequences of a stay-green mutation on tissue and cellular physiology.

RESULTS

Total Flavedo Pigment Content

A mutant was identified among a population of *C. sinensis* trees whose fruit developed a dark brown external color upon ripening, rather than the characteristic orange of the wild type (Fig. 2A). This coloration was confined to the flavedo (Fig. 2B), and no other unusual phenotypes were observed in either the fruit, which were typically green at preripe stages, or vegetative tissues. In order to determine the molecular basis of the abnormal coloration, pigment levels in the flavedo of the *nan* mutant were compared with those from wild-type fruit at a range of developmental and ripening stages, spanning 120 to 275 DPA. The wild-type and *nan* fruit showed no differences in the levels of total Chls or carotenoids at the immature and mature green stages (120–180 DPA; Fig. 2, C and D). The apparent Chl depletion in *nan* and wild-type fruit prior to ripening (120–180 DPA; Fig. 2C) reflects a dilution effect due to cell expansion in the fruit peel (Bain, 1958) rather than Chl degradation, since the ratio of dry weight to fresh weight decreased from 0.30 to 0.14 in the wild type and from 0.32 to 0.16 in *nan*, resulting in a slight increase in the total amount of Chl (694 ± 42 to 772 ± 32 $\mu g\ g^{-1}$ dry weight in the wild type and 733 ± 122 to 752 ± 68 $\mu g\ g^{-1}$ dry weight in *nan*). However, while the abundance of Chl decreased during ripening to barely detectable levels in wild-type fruit, this did not occur in *nan*, and the levels remained unchanged (Fig. 2C) after natural color break (224 DPA). Furthermore, although both varieties showed a characteristic increase in carotenoid levels during ripening, consistent with the development of orange color, they were substantially higher in *nan* fruit and were approximately double those of the wild type at the fully ripe stage (275 DPA; Fig. 2D).

Measurement of Chls, Derivatives, and CLH Activity

The levels of Chls and their derivatives in the flavedo of both varieties were analyzed by HPLC at three developmental stages: mature green (180 DPA), breaker (224 DPA), and ripe (248 DPA; Table I). The concentrations of Chl *a* (105–120 $\mu g\ g^{-1}$ fresh weight) and Chl *b* (17–23 $\mu g\ g^{-1}$ fresh weight) showed a typical dramatic decrease during ripening in the wild type ($\leq$98%) but remained high in *nan*, with almost no Chl degradation. Moreover, Chl dephytylated compounds (chlorophyllides and pheophorbides), which typically accumulate in PaO-affected stay-green mutants during ripening, were not detected in either *nan* or wild-type flavedo at any stage (Table I; Supplemental Fig. S1). Both varieties had similarly low levels of OH-Chl *a*, pheophytin *a*, and OH-Chl *b* (Table I), although the

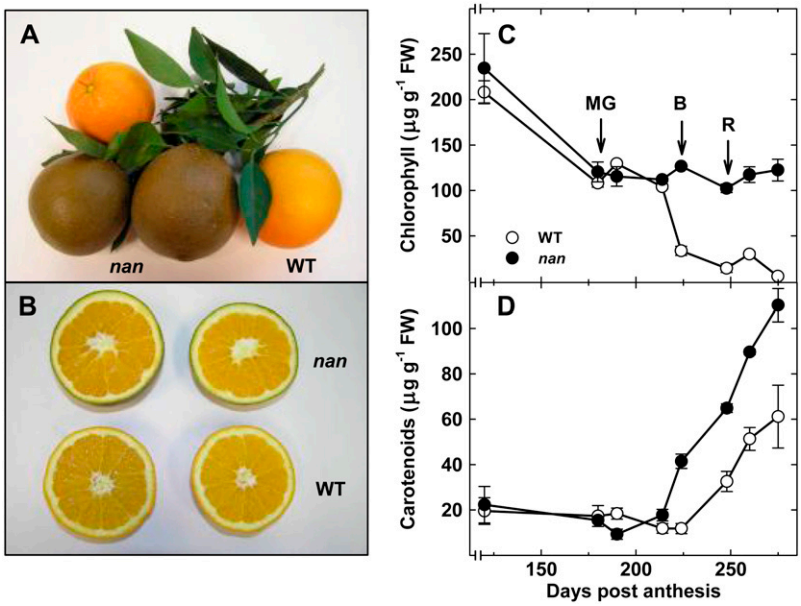

Figure 2. External (A) and internal (B) appearance of wild-type and *nan* fruits at a fully ripe stage (275 DPA), and quantification of total Chls (C) and carotenoids (D) in the flavedo of *C. sinensis* 'Washington Navel' (WT; wild type; white circles) and *nan* (black circles) during fruit ripening. Data are means $\pm$ SE ($n = 3$). Error bars smaller than the symbol size are not visible. MG, Mature green stage (180 DPA); B, breaker stage (224 DPA); R, ripe stage (248 DPA). FW, Fresh weight.

oxidized Chls were always more abundant in *nan* fruit. Despite the lack of Chl degradation in *nan*, no major differences were detected in CLH activity between the wild type and *nan* in mature green or breaker fruits; indeed, CLH activity was significantly higher in ripe *nan* fruit (Table I).

Expression of Genes Involved in Pigment Biosynthesis and Degradation

The expression levels of a selection of genes associated with pigment biosynthesis and catabolism were quantified by real-time reverse transcription (RT)-PCR during fruit development and ripening in the flavedo of wild-type and *nan* fruit (Fig. 3). These included *PHYTOENE SYNTHASE* (*PSY*), the first committed step in the carotenoid biosynthesis pathway (Fraser et al., 2002); *CHL P*, a gene involved in the biosynthesis of the phytyl chain of Chls (Tanaka et al., 1999); and two Chl catabolic genes, *PaO* and *RCCR*. Expression of *PSY* increased rapidly in both wild-type and *nan* flavedo, although maximal expression in the wild type was seen at the breaker stage, after which *PSY* transcript abundance decreased, while expression continued to increase during ripening in *nan*, peaking at the ripe stage, before decreasing during overripening. The expression patterns of the genes involved in Chl biosynthesis and degradation were similar in the wild type and *nan* in terms of both relative abundance and changes during fruit development (Fig. 3, B–D).

Effect of Ethylene on Pigment Composition and Gene Expression

The plant hormone ethylene is known to promote Chl degradation in the citrus flavedo (García-Luis et al., 1986; Jacob-Wilk et al., 1999), so this phenomenon was examined in the *nan* mutant to determine whether the mutant phenotype might be associated with ethylene insensitivity. To this end, mature green wild-type and *nan* fruits were treated with 10 μL L^{-1} ethylene for 72 h, then total Chl and carotenoid levels were assayed and *PaO*, *CHL P*, *PSY*, and *CLH* expression was analyzed in flavedo tissues (Fig. 4). As expected, the ethylene treatment induced a substantial decrease in total Chl concentration in the wild-type flavedo (approximately 50 μg g^{-1} fresh weight, which represents almost half of the initial content), while no significant change was detected in the *nan* flavedo (Fig. 4A). However, the expression patterns of *PaO*, *CHL P*, *PSY*, and *CLH* showed similar changes in both varieties in response to the ethylene treatment (Fig. 3B), indicating that *nan* is ethylene responsive but that this response is upstream of, or independent from, the signaling pathway that induces Chl degradation. Furthermore, the treatment did not alter total carotenoid content (Fig. 4A), although *PSY* expression increased to the same degree in both varieties (Fig. 4B).

Comparative Transcriptome Profiling

In order to gain insight into the potential basis and consequences of the stay-green phenotype, a survey of transcript expression in wild-type and *nan* flavedo was made using a 7,000-element citrus cDNA microarray (Forment et al., 2005). Pairwise analyses of RNA extracts from wild-type and *nan* flavedo tissue at the mature green, breaker, and ripe stages identified 11 distinct genes that were differentially expressed in all three stages, of which five could be annotated based on sequence homology tBLASTx searches against the National Center for Biotechnology Information (NCBI) nonredundant database (Table II). The only EST that showed down-regulation in the *nan* flavedo at all three developmental stages was a predicted *SGR* gene homolog, with the highest degree of similarity to an *SGR* gene from tomato (Table II). In the *nan* mutant, three other genes, annotated as a miraculin-like protein 2 gene, a secretory peroxidase gene, and a guanyl-nucleotide exchange factor gene, showed up-regulation at the green stage and subsequent down-regulation (Table II). In contrast, the expression level of a Cys protease gene was lower during the green stage but higher at the breaker and ripe stages (Table II). No significant se-

Table I. *Chl, Chl derivative, and CLH activity in the flavedo of wild-type citrus and the nan stay-green mutant at mature green (180 DPA), breaker (224 DPA), and ripe (248 DPA) stages*

ND, Not detected. Data are means ± SE (n = 3).

Variable	Mature Green Stage		Breaker Stage		Ripe Stage	
	Wild Type	*nan*	Wild Type	*nan*	Wild Type	*nan*
Pigments (μg g^{-1} fresh weight)						
Chl *a*	105.35 ± 8.25	120.32 ± 5.21	2.64 ± 0.03	100.65 ± 2.64	1.05 ± 0.01	105.34 ± 9.65
OH-Chl *a*	0.52 ± 0.02	1.42 ± 0.11	ND	0.99 ± 0.02	ND	5.21 ± 0.02
Pheophytin *a*	2.01 ± 0.01	1.75 ± 0.05	0.09 ± 0.01	0.68 ± 0.06	0.40 ± 0.04	0.65 ± 0.11
Chl *b*	23.51 ± 1.57	16.57 ± 0.08	0.83 ± 0.01	21.36 ± 1.12	ND	9.65 ± 0.54
OH-Chl *b*	ND	ND	ND	ND	ND	1.06 ± 0.09
Total Chls	131.39 ± 8.64	140.24 ± 15.36	3.56 ± 0.46	123.68 ± 3.21	0.07 ± 0.01	120.85 ± 8.24
Chlorophyllide *a*	ND	ND	ND	ND	ND	ND
Pheophorbide *a*	ND	ND	ND	ND	ND	ND
CLH activity (μmol h^{-1} g^{-1} fresh weight)	4.5 ± 0.3	4.4 ± 0.3	2.4 ± 0.1	2.1 ± 0.1	1.8 ± 0.2	2.4 ± 0.2

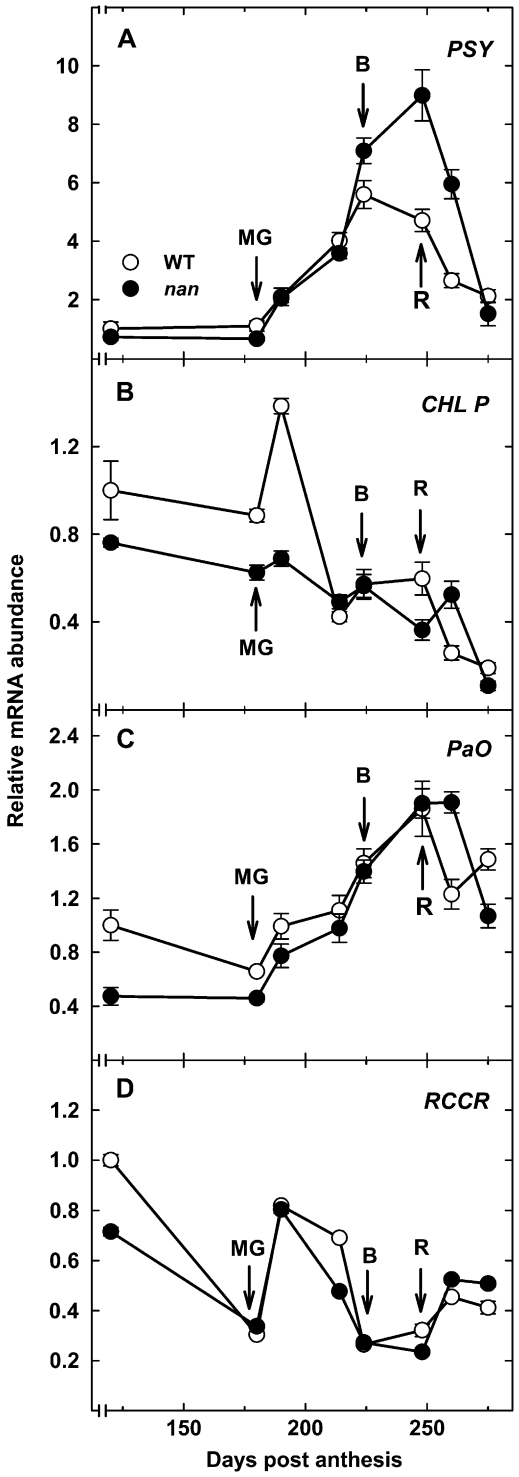

Figure 3. Expression analysis by real-time RT-PCR of transcripts in the flavedo of the wild type (white circles) and the *nan* mutant (black circles) of *PSY* (A), *CHL P* (B), *PaO* (C), and *RCCR* (D) during fruit growth and ripening. An expression value of 1 was arbitrarily assigned to the 120-DPA wild-type sample. MG, Mature green stage (180 DPA); B, breaker stage (224 DPA); R, ripe stage (248 DPA). Data are means ± SE ($n = 3$). Error bars smaller than the symbol size are not visible.

quence homology was apparent for the other six ESTs (CX299753, CX306150, CX299918, CX299940, CX287589, and CX289503), and, other than CX289503, which was expressed at higher levels in *nan* at all three stages, they exhibited similar relative expression patterns, with elevated transcript levels in the mutant flavedo at the mature green stage but reduced expression at the breaker and ripe stages (data not shown).

Since mutations in the *SGR* gene are responsible for the phenotypes of several stay-green mutants (Armstead et al., 2007; Jiang et al., 2007; Park et al., 2007; Ren et al., 2007; Sato et al., 2007), a 1.2-kb genomic region, including the promoter and coding regions, of the citrus *SGR* gene was cloned from wild-type and *nan* genomic DNA (GenBank accession no. AM922109), but differences were not observed. Furthermore, to determine whether a deletion in one or more copies of the *SGR* gene could be responsible for the *nan* phenotype, the relative gene dosage of *SGR* was assessed in wild-type and *nan* fruit by real-time PCR using genomic DNA, and again no difference was observed (data not shown).

In addition to the 11 genes that showed differences in transcript abundance at all three stages, a broader group of genes showed significantly different expression levels at one or two stages (Supplemental Table S1). The annotated functions of these genes, which are divided into several classes in Tables III and IV, and their collective expression patterns, suggest two key trends. First, at the mature green stage, a range of genes encoding components of the photosynthetic machinery and ancillary proteins associated with photosynthesis (e.g. NADPH:protochlorophyllide oxidoreductase, Chl *a*/*b*-binding protein [Cab], subunits of PSI and PSII, and Rubisco subunit-binding protein) were expressed at substantially lower levels in *nan*. Second, many genes associated with abiotic stress, and particularly responses to high light and oxidative stress, were upregulated in *nan* at both the mature green (Table III) and ripe (Table IV) stages. These included genes involved in the synthesis of compounds that ameliorate the effects of oxidative stress and reactive oxygen species (ROS), such as phenylpropanoids, polyamines, and carotenoids, and with the synthesis of jasmonic acid, salicylic acid, and ethylene, which have well-established connections with biotic and abiotic stress-mediated signaling. To further verify that the *nan* phenotype is associated with increased oxidative stress, the concentration of ascorbic acid, an antioxidant compound that accumulates in response to oxidative stress in many plant species (Mitler et al., 2004), including citrus (Iglesias et al., 2006), was measured in extracts from wild-type and *nan* ripe flavedo. As predicted, ascorbic acid levels in ripe fruit flavedo were significantly greater in *nan* than in the wild type (0.43 ± 0.04 and 0.29 ± 0.02 mg g^{-1} fresh weight, respectively).

In addition to these defined functional categories, a diverse set of genes with previously reported associations with oxidative stress showed differential ex-

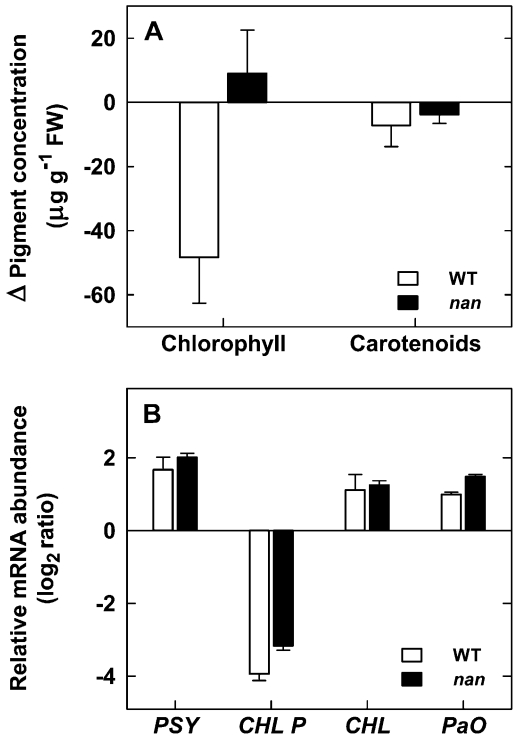

Figure 4. Effects of ethylene treatments on both total pigment composition (A) and changes in mRNA abundance (B) in the flavedo of wild-type (white columns) and *nan* (black columns) fruits. Fruits were treated with 10 μL L^{-1} ethylene in controlled-atmosphere postharvest chambers at 20°C for 72 h. Pigment content was expressed as the absolute increment between control and treated samples. Transcript abundance of *PSY*, *CHL P*, *CHL*, and *PaO* was determined by real-time RT-PCR. The expression ratio between treated and untreated fruits was calculated and $\log_2$ transformed. All data are means ± SE ($n = 3$).

pression between the varieties (Tables III and IV). For all putative functional categories, where a link between the apparent Arabidopsis ortholog of the citrus gene on the microarray and oxidative stress has been described in the literature, the corresponding reference is cited in Tables III and IV.

To validate the microarray results, quantitative RT-PCR analyses were performed on genes that represented different general patterns of expression (Table II) at the mature green, breaker, and ripe developmental stages. Specifically, these comprised representatives of genes that in the *nan* mutant either showed reduced expression at all three stages (*SGR*), higher expression at the mature green stage and then reduced expression during ripening (secretory peroxidase gene), or reduced expression in mature green fruits and increased transcript levels in ripening fruit (Cys protease gene). In all cases, the expression patterns (Fig. 5) were essentially identical to those obtained with the microarray.

2D-DIGE Analysis of Protein Expression

In a parallel analysis, and to complement the microarray study, a comparative proteomic survey was performed on the wild-type and *nan* flavedo at the same three stages using 2D-DIGE (Rose et al., 2004). The gel comparisons revealed 13 protein spots that were consistently differentially expressed between *nan* and the wild type in all replicate analyses (arrows in representative gels shown in Supplemental Fig. S2). Differentially expressed spots were defined as those with a volume ratio above or below the 2-fold SD threshold, based on the normalized model curve of the spot volume ratio data set. Subsequent analyses by liquid chromatography-electrospray ionization-tandem mass spectrometry, followed by an interrogation of the NCBI nonredundant Green Plant database with the mass spectra using the Mascot search engine, identified a subset of 11 proteins (corresponding to those labeled 1–11 in Supplemental Fig. S2) with high confidence identification and annotation (Table V). These comprised a manganese superoxide dismutase, a copper zinc superoxide dismutase, the Rubisco large subunit (two spots), two heat shock proteins (HSP19 and HSP21), a lectin-related protein, a Gly-rich RNA-binding protein, a copper chaperone, an early light-induced protein (ELIP), and a protein with unknown function (gi|8778393). At the mature green stage, the only proteins that were detected with reduced expression in *nan* were HSP21 and the putative Gly-rich protein. HSP21, a protein involved in the chloroplast-to-chromoplast transition of tomato fruits (Neta-Sharir et al., 2005), was consistently less abundant in all three

Table II. *Genes showing significant expression changes in the flavedo of the wild type and the nan stay-green mutant at all three stages studied: mature green (180 DPA), breaker (224 DPA), and ripe (248 DPA) stages*

Differences in gene expression of at least 2-fold ($P \leq 0.001$) in each of three replicates were considered to be statistically significant.

Citrus EST Accession No.	tBLASTx Best Hit	Identities[a]	Arabidopsis Ortholog	Mature Green $\log_2$ Ratio[b]	Breaker $\log_2$ Ratio[b]	Ripe $\log_2$ Ratio[b]
CX308230	SGR protein (*Solanum lycopersicum*)	86%	At4g22920	−1.97 ± 0.11	−1.71 ± 0.12	−1.67 ± 0.11
CX305230	Miraculin-like protein 2 (*Citrus jambhiri*)	96%	At1g17860	1.08 ± 0.17	−1.72 ± 0.18	−1.30 ± 0.17
CX308252	Secretory peroxidase (*Nicotiana tabacum*)	89%	At4g21960	2.19 ± 0.16	−1.02 ± 0.18	−2.76 ± 0.16
CX302192	Guanyl-nucleotide exchange factor (*Arabidopsis thaliana*)	71%	At1g01960	1.99 ± 0.14	−2.14 ± 0.15	−1.02 ± 0.14
CX305503	Cys proteinase (*Citrus sinensis*)	100%	At4g32940	−1.05 ± 0.20	1.42 ± 0.21	1.52 ± 0.20

[a]Identities at the amino acid level. [b]Induction fold values are expressed as log-transformed mean ratios of *nan* to wild-type expression.

Table III. *Examples of genes showing different expression levels in the flavedo of wild-type or nan stay-green mutant fruits at mature green stage (180 DPA), as determined with a citrus microarray, highlighting those associated with oxidative stress, chloroplast function, or senescence*

References describing such an association for the Arabidopsis ortholog of the citrus gene are indicated. Differences in gene expression of at least 2-fold ($P \leq 0.001$) in each of three replicates were considered to be statistically significant.

Functional Class	Best BLAST Hit	Higher Expression		Citrus EST Accession No.	Arabidopsis Ortholog	Related References
		Wild Type	*nan*			
Primary metabolism	Plastidic Glc-6-P dehydrogenase		X	CX293894	At5g13110	Debnam et al. (2004)
	Chloroplastic Asp aminotransferase		X	CX294238	At2g22250	de la Torre et al. (2006)
	Asp synthetase	X		CX306022	At3g47340	Lam et al. (1998)
Photosynthesis, light signaling	RPT2		X	CX300991	At2g30520	Inada et al. (2004)
	NADH:protochlorophyllide oxidoreductase	X		CX289541	At5g54190	Rossel et al. (2002)
	PSI subunit L	X		CX287010	At4g12800	Kimura et al. (2003)
	PSI subunit E	X		CX300489	At2g20260	
	Putative PSI subunit	X		CX299745	At4g02770	Kimura et al. (2003)
	Cab 3	X		CX287196	At1g29910	Kimura et al. (2003)
	PSII type I Cab	X		CX300355	At2g34430	Kimura et al. (2003)
	Lhcb2 protein	X		CX300473	At3g27690	Kimura et al. (2003)
	Lhcb6 protein	X		CX300344	At1g15820	Rossel et al. (2002)
	Lhca2	X		CX300483	At3g61470	Kimura et al. (2003)
	Rubisco subunit-binding protein (chaperonin)	X		CX300392	At2g28000	Tosti et al. (2006)
ROS, redox	Secretory peroxidase		X	CX308252	At4g21960	
	FAD-linked oxidoreductase	X		CX292465	At5g44380	Kim et al. (2005)
	Metallothionein protein	X		CX303735	At3g15353	Guo et al. (2004)
Phenylpropanoids	Phe-ammonia lyase		X	CX308098	At2g37040	Rossel et al. (2002)
	Chalcone synthase		X	CX308007	At5g13930	Rossel et al. (2002)
	Flavonol 3′-*O*-methyltransferase		X	CX308025	At5g54160	Kimura et al. (2003)
	Coumarate 3-hydroxylase		X	CX290216	At2g40890	
Polyamines	SAM decarboxylase		X	CX308026	At3g02470	Guo et al. (2004)
Protein stability	Chloroplastic heat shock protein	X		CX292078	At4g27670	
	HSP20	X		CX309295	At2g29500	Kim et al. (2005)
	Heat shock protein		X	CX294165	At3g52490	
Defense	Chitinase	X		CX292066	At3g54420	
Miscellaneous	β-Amylase		X	CX291892	At3g23920	Rossel et al. (2002)
	UVI-1 homolog		X	CX301008	At1g19020	Gadjev et al. (2006)
	Gly-rich RNA-binding protein	X		CX287915	At3g26740	Kimura et al. (2003)

stages (−5.5, −3, and −2.7-fold at the mature green, breaker, and ripe stages, respectively). Conversely, the two superoxide dismutases and the copper chaperone protein were upregulated in *nan* at the mature green stage. The two spots of the Rubisco large subunit and the lectin-related precursor were less abundant in *nan* at the breaker and ripe stages, while ELIP and HSP19 were expressed at higher levels than in the wild type during ripening (Table V). This was particularly noticeable with ELIP, which was on average expressed at 14-fold higher levels in *nan* at the ripe stage.

The 2D-DIGE screens were further validated by western-blot analysis of protein extracts from the flavedo of wild-type and *nan* fruits at all three stages with a Rubisco antiserum. The immunoblot analysis indicated that the Rubisco large subunit and small subunit were expressed at lower levels in *nan*, in agreement with the 2D-DIGE analysis, and that protein abundance declined during ripening (Fig. 6; Table V). It should be noted that cDNAs for the Rubisco large subunit were not represented on the citrus microarray, but those for the small subunit were present and the array analysis indicated that expression was statistically lower in breaker fruit. However, data generated by similar analyses with RNA from the mature green and ripe stages did not reach the *P* value threshold for a statistically significant comparison (Supplemental Table S1).

The 2D-DIGE data were compared with the microarray study in an attempt to identify targets that were common to both analyses. Most of the microarray elements corresponding to the 10 proteins (other than Rubisco) found in the 2D-DIGE study either did not generate expression data with significant *P* value thresholds in the microarray analyses or were not represented on the array. Thus, only two differentially expressed putative unigenes in the citrus chip matched a high-confidence best hit from the proteomic analyses (Table V; Supplemental Fig. S2): a lectin-related protein and HSP19. For the lectin-related protein, statistically

Table IV. *Examples of genes showing different expression levels in the flavedo of wild-type or nan stay-green mutant fruits at the ripe stage (248 DPA), as determined with a citrus microarray, highlighting those associated with oxidative stress, chloroplast function, or senescence*

References describing such an association for the Arabidopsis ortholog of the citrus gene are indicated. Differences in gene expression of at least 2-fold ($P \leq 0.001$) in each of three replicates were considered to be statistically significant.

Functional Class	Best BLAST Hit	Higher Expression		Citrus EST Accession No.	Arabidopsis Ortholog	Related References
		Wild Type	*nan*			
Primary metabolism	Trp synthase		X	CX291092	At5g54810	Zhao et al. (1998)
Photosynthesis, light signaling	Lhcb2 protein		X	CX200280	At2g05100	Kimura et al. (2003)
ROS, redox	Cytochrome bf_6 complex subunit		X	CX37372	At2g26500	Kimura et al. (2003)
	GST1		X	CX301042	At2g30860	Rossel et al. (2002)
	GST6	X		CX288839	At2g47730	Rossel et al. (2002)
	Peroxidase	X		CX308204	At4g21960	Wong et al. (2006)
	Ascorbate oxidase	X		CX289525	At5g21100	Yamamoto et al. (2005)
Phenylpropanoids	Isoflavone reductase-like		X	CX308502	At4g39230	
	Flavonol 3′-*O*-methyltransferase		X	CX289068	At5g54160	Kimura et al. (2003)
Polyamines	SAM decarboxylase		X	CX289919	At3g25570	Guo et al. (2004)
Isoprenoids, carotenoids	Geranylgeranyl diphosphate synthase		X	CX290062	At3g14510	
Salicylic acid	SAM-dependent methyltransferase		X	CX308455	At3g11480	Chen et al. (2003)
Jasmonic acid	Lipoxygenase (LOX3)		X	CX288539	At1g17420	Mahalingam et al. (2005)
Ethylene	ACC oxidase		X	CX292573	At1g05010	Gadjev et al. (2006)
Defense	Chitinase	X		CX291879	At3g12500	Bray (2002)
Miscellaneous	Miraculin	X		CX306063	At1g17860	Rizhsky et al. (2004)
	Cys protease (SAG12)		X	CX287658	At5g45890	Guo et al. (2004)
	Glycosyltransferase		X	CX288595	At3g11340	Gadjev et al. (2006)
	Glu decarboxylase		X	CX288553	At5g17330	
	Vacuolar processing enzyme		X	CX287419	At4g32940	Gepstein et al. (2003)

significant data in the two surveys indicated repression in the *nan* mutant of both mRNA (Supplemental Table S1) and protein (Table V) at the ripe stage. However, for HSP19, transcript abundance was lower in *nan* at the mature green stage (Supplemental Table S1), while protein levels appeared to be higher (Table V) at the ripe stage.

Gene Expression of ELIP

The transcript levels corresponding to ELIP, the protein with the greatest difference in expression between wild-type and *nan* flavedo (Table V), were quantified in the two varieties by real-time RT-PCR (Fig. 7). Expression of *ELIP* in the wild type was relatively low until the breaker stage (214 DPA), when levels increased dramatically, before peaking at the ripe stage and declining thereafter. In contrast, *ELIP* mRNA levels increased earlier in *nan*, prior to the breaker stage, and similarly declined somewhat earlier than the wild type during ripening.

DISCUSSION

The most striking phenotype of the *nan* mutant, which resulted in its initial identification, is the unusual brown color of the flavedo in the ripe fruit (Fig. 2A). An evaluation of the flavedo pigment composition indicated that *nan* can be defined as a type C stay-green variant (Thomas and Howarth, 2000), since Chl levels remained elevated during ripening rather than showing a typical decrease, while other ripening-related processes, such as carotenoid synthesis, proceeded normally (Fig. 2A; Table I). The brown coloration of *nan* fruit thus reflects the cumulative accumulation of Chl and carotenoids. This is further evidenced by the observation that *PaO*, *RCCR*, and *CHL P* transcript levels remained relatively constant, or showed only small decreases, during this period (Fig. 3, B–D).

Descriptions of stay-green mutants with major reductions in PaO activity from a range of plant species consistently report the accumulation of dephytylated intermediates in the Chl catabolic pathway during senescence (Hörtensteiner, 2006), and specifically elevated levels of pheophorbide *a* (Vicentini et al., 1995; Thomas et al., 1996; Roca et al., 2004), while no such accumulation has been detected in corresponding wild-type plants. These stay-green mutants are therefore impaired in particular steps in Chl degradation, rather than showing down-regulation of the entire pathway. To compare *nan* with the previously characterized stay-green mutants, and to determine whether there are similarly distinct defects in specific steps in Chl catabolism, we measured the levels of Chl, Chl dephytylated compounds, and CLH activity in the flavedo of *nan* and wild-type fruits (Table I). Neither contained detectable levels of chlorophyllides or pheophorbides, although oxidized Chl derivatives were

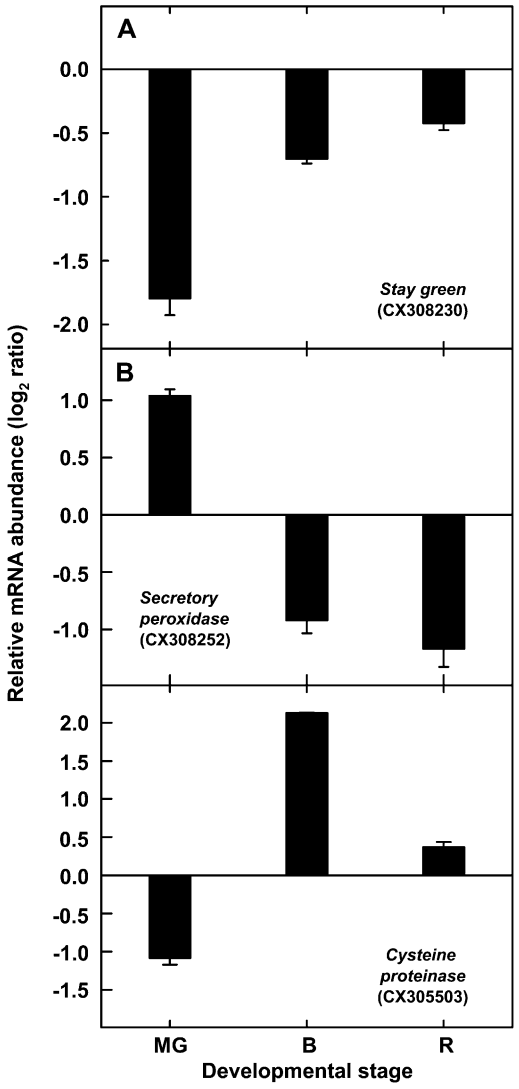

Figure 5. Relative gene expression in the flavedo of wild-type and *nan* fruits of *SGR* (A), secretory peroxidase gene (B), and Cys protease gene (C) transcripts determined by real-time RT-PCR. MG, Mature green stage (180 DPA); B, breaker stage (224 DPA); R, ripe stage (248 DPA). Log_2-transformed mean ratios of *nan* to wild-type expression ± SE are presented ($n = 3$). GenBank accession numbers of the ESTs are indicated in parentheses.

present in both varieties. Relatively low levels of OH-Chl *a* were measured at the mature green stage in wild-type and *nan* fruits, but they were only detected in the mutant at the ripe stage and OH-Chl *b* was also only observed in ripe *nan* flavedo. The accumulation of such hydroxylated Chl derivatives has been noted previously in several stay-green mutants and has been attributed to nonspecific oxidation resulting from the elevated Chl levels, although the exact mechanism leading to their production is unknown (Roca and Mínguez-Mosquera, 2006). The patterns of CLH activity (Table I) and *PaO* and *RCCR* gene expression (Fig. 2) were similar in both varieties, and the patterns of expression of *PSY*, *CHL P*, and *PaO* were in close agreement with similar studies of other citrus species (Alós et al., 2006).

The response of the *nan* mutant to ethylene was also evaluated, since this hormone regulates leaf senescence (Kao and Yang, 1983; Choe and Whang, 1986) and color change in many fruit species, including citrus, through the activation of Chl degradation (García-Luis et al., 1986; Trebitsh et al., 1993; Jacob-Wilk et al., 1999) and carotenoid biosynthesis (Young and Jahn, 1972; Eilati et al., 1975). The results indicated that rapid ethylene-induced Chl loss was impaired in the *nan* mutant (Fig. 4), as has been reported previously in tomato and soybean stay-green mutants (Guiamét and Giannibelli, 1994; Akhtar et al., 1999). However, *nan* is ethylene responsive, because ethylene-induced gene expression, including transcripts involved in Chl synthesis and degradation or carotenoid biosynthesis, was similar in both varieties. While *PSY* expression was upregulated in *nan* and the wild type (Fig. 4B), the time course of the analysis was not sufficiently long to generate significant changes in carotenoid levels (Fig. 4A).

These data suggest that the *nan* mutation is not directly related to a single disruption in any of the principal established enzymatic steps (CLH, PaO, and RCCR) of Chl catabolism and is thus distinct from previously reported stay-green mutants. This hypothesis was explored by profiling transcript expression in the flavedo of wild-type and *nan* fruit at the mature green, breaker, and ripe stages. It was reasoned that genes whose expression was disrupted throughout fruit ontogeny might be more directly related to the function of the *nan* mutation, while those that showed differential expression only at later ripening stages might reflect secondary effects. Therefore, particular attention was paid to identifying transcripts with significantly different expression levels at all three stages. Interestingly, of the 11 genes that matched this criterion, the only one that was consistently downregulated was an *SGR* homolog that appears to be orthologous to Arabidopsis *SGR1* (Table II). Cloning and sequencing of the citrus *SGR* gene revealed no differences between the wild type and *nan*, and no difference in gene dosage was detected in the two varieties. Taken together, the lack of Chl catabolite accumulation and the suppressed expression of the citrus *SGR* gene suggest that the *nan* mutation is associated with an early regulatory step that modulates *SGR* expression, rather than directly exerting a downstream effect on a specific aspect of catabolism.

In addition to characterizing the potential basis of the *nan* mutation, comparative transcriptomic and proteomic profiling were performed to assess the consequences of a stay-green mutation on flavedo tissue physiology and to provide insights into the metabolic pathways that are affected. To date, the only reported attempt at a larger scale study of differential gene expression in a stay-green mutant focused on three genes (Rubisco activase, soluble starch synthase, and

Table V. *Relative changes in the abundance of 11 protein spots in the flavedo of wild-type and nan mutant fruits at mature green (180 DPA), breaker (224 DPA), and ripe (248 DPA) stages, as determined using 2D-DIGE*

Differentially expressed spots were defined as those with a volume ratio above or below the 2 SD threshold based on the normalized model curve of the spot volume ratio data set. Protein annotation was performed after a search in the NCBI nonredundant Green Plant database. The accession numbers and corresponding protein scores are listed. Data are means ± SE ($n = 4$) of the normalized spot volume *nan* to wild-type ratio. Arrows (→) indicate no significant changes in relative protein abundance.

Spot	Accession No.	Best Hit	Protein Score	Fold Change		
				Mature Green	Breaker	Ripe
1	gi|54292100	Manganese superoxide dismutase (*Camellia sinensis*)	103	2 ± 0.05	2 ± 0.2	→
2	gi|14158	Heat shock protein 21 (*Petunia* × *hybrida*)	101	−5.5 ± 2.1	−3.0 ± 0.6	−2.7 ± 0.6
3	gi|30039180	Copper chaperone (*Solanum lycopersicum*)	53	4.8 ± 0.5	→	→
4	gi|2274917	Copper/zinc superoxide dismutase (*Citrus sinensis*)	61	5 ± 0.3	→	7.1 ± 0.7
5	gi|6911142	Gly-rich RNA-binding protein 1 (*Catharanthus roseus*)	42	−7.4 ± 0.1	→	→
6	gi|4206520	Ribulose-1,5-bisphosphate carboxylase (*Severinia buxifolia*)	851	→	−2.2 ± 0.1	−2.7 ± 0.1
7	gi|4206520	Ribulose-1,5-bisphosphate carboxylase (*Severinia buxifolia*)	711	→	−2.3 ± 0.1	−3.4 ± 0.1
8	gi|11596188	Lectin-related protein precursor (*Citrus* × *paradisi*)	329	→	−3.8 ± 0.6	−3.2 ± 1.0
9	gi|7447856	Early light-inducible protein precursor (*Glycine max*)	56	→	6.6 ± 0.7	14 ± 3.7
10	gi|8778393	F16A14.17 (*Arabidopsis thaliana*)	47	→	2.8 ± 0.6	→
11	gi|30575572	HSP19 class I (*Citrus* × *paradisi*)	168	→	→	2.8 ± 0.02

Gly decarboxylase genes), which were identified through a differential display screen of a durum wheat stay-green mutant (Rampino et al., 2006). These genes, together with those for the Rubisco small subunit and Cab, were expressed at higher levels or underwent a slower decline in abundance during senescence in the mutant. In addition, a study of the stay-green *green flesh* tomato mutant suggested that the expression of several photosynthesis-related transcripts, or their cognate proteins, underwent a slower decrease in abundance in senescing leaves of the mutant than the wild type (Akhtar et al., 1999). Global transcript expression was monitored in the flavedo of *nan* and wild-type fruit at the mature green and ripe stages to identify genes that were up- or down-regulated in the mutant. Published Arabidopsis microarray data were then analyzed manually, or using tools such as Genevestigator (www.genevestigator.ethz.ch), to identify developmental processes or stimuli that similarly influence transcript accumulation of the Arabidopsis orthologs of the differentially expressed citrus clones. A similar procedure was followed using differentially expressed proteins (Table V).

One particularly clear trend that emerged from the analysis was that a broad set of photosynthesis-related genes and proteins were downregulated in *nan* at the mature green stage (Tables III and IV), a phenomenon that is closely associated with high light-induced stress (Rossel et al., 2002; Kimura et al., 2003). Plants can adjust the size of the light-harvesting antenna complex under such conditions, and it is thought that this occurs in order to reduce the production of ROS, which are generated under excess light conditions (Escoubas et al., 1995; Heddad and Adamska, 2000). Oxidative stress-inducing treatments have also been reported to trigger the down-regulation of photosynthesis-associated genes (Tosti et al., 2006); thus, there appears to be feedback between cellular redox status

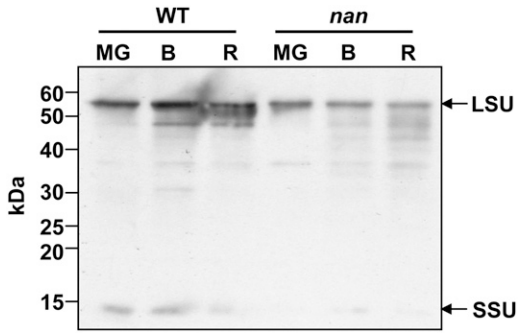

Figure 6. Immunoblot analysis of Rubisco expression in flavedo of wild-type and *nan* fruits. Bands corresponding to the large subunit (LSU) and the small subunit (SSU) are highlighted. MG, Mature green stage (180 DPA); B, breaker stage (224 DPA); R, ripe stage (248 DPA). Molecular mass markers are indicated.

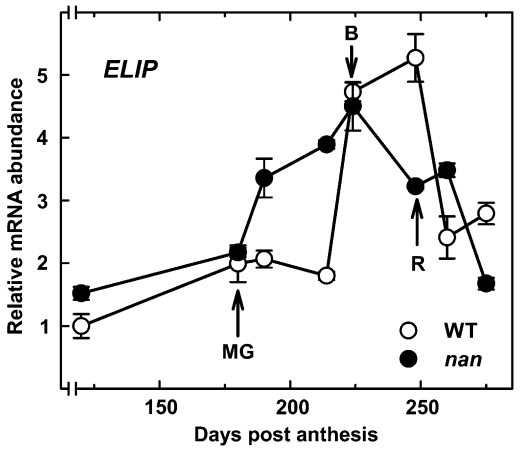

Figure 7. Transcript levels of the *ELIP* gene during fruit growth and ripening in the flavedo of wild-type (white circles) and *nan* (black circles) fruits. Analyses were performed by real-time RT-PCR, and an expression value of 1 was arbitrarily assigned to the 120-DPA wild-type sample. MG, mature green stage (180 DPA); B, breaker stage (224 DPA); R, ripe stage (248 DPA). Data are means ± SE ($n = 3$). Error bars smaller than the symbol size are not visible.

and oxidative stress that represses photosynthetic function. In addition, the proteomic analysis identified rbcL as one of the major proteins with lower abundance in *nan* (Figs. 5 and 6; Table V), which differs from the results seen with a rice *sgr* mutant (Sato et al., 2007) and the retention of Rubisco in leaves of the tomato *green flesh* mutant (Akhtar et al., 1999) but agrees with the previously observed reduced Rubisco protein levels in a *P. vulgaris* stay-green mutant (Bachmann et al., 1994).

If photosynthetic capacity is insufficient under conditions of excess absorbed light, free Chl can generate ROS, which in turn can cause extensive oxidative damage to the thylakoid membrane (Barber and Andersson, 1992; Niyogi, 1999). Accordingly, a second pattern that emerged from the proteomic and transcriptomic profiling was the association of genes that were among the most substantially up- or down-regulated in *nan* with abiotic stress, and specifically with high light or oxidative stress (Tables III and IV; Supplemental Table S1). While it is not practical to describe all the relevant genes and biochemical or physiological processes here, examples are shown in Tables III and IV, together with associated reports in the literature linking the specific Arabidopsis orthologs with stress responses or senescence. The *nan* flavedo had elevated levels of transcripts or proteins associated with enzymatic mechanisms for scavenging ROS, such as superoxide dismutase, and the biosynthesis of phenylpropanoids, polyamines, and isoprenoids, which provide nonenzymatic antioxidative protection (Jordan, 2002; Apel and Hirt, 2004; Kuehn and Phillips, 2005). Furthermore, the elevated carotenoid levels, higher ascorbic acid content, and higher levels of OH-Chls in *nan* after the breaker stage of ripening (Fig. 2) were likely a response to ROS, as reported previously (Bouvier et al., 1998; Mitler et al., 2004). Another set of pathways that showed apparent upregulation in *nan* were those leading to the synthesis of ethylene, jasmonic acid, and salicylic acid (Table III). While these hormones have a well-established role in regulating defense responses following microbial challenge, there is increasing evidence that they are involved in substantial cross talk between biotic and abiotic stress pathways and ROS-triggered molecular events (Fujita et al., 2006).

The comparative proteomic analyses also provided insights into the diversity of processes that were influenced by the *nan* mutation and, importantly, revealed different gene targets from the microarray analyses; therefore, the two approaches were complementary. The only identified protein that was expressed at lower levels in all three stages (Table V) was HSP21, a heat shock protein with chaperone-like activity (Lee et al., 1997). Although its biochemical function in fruit has yet to be fully elucidated, this chloroplastic protein has proposed roles in the protection of PSII from photooxidative stress and in the conversion of chloroplasts to chromoplasts during fruit ripening (Neta-Sharir et al., 2005). The reduced expressed of HSP21 in *nan*, therefore, may be associated with the abnormal levels of Chl or altered plastid ontogeny in the mutant, for example, if it participates in the disassembly of thylakoid membrane proteins and binding to partially folded or denatured proteins (Sun et al., 2002).

In contrast, the protein that showed the most relatively elevated expression in *nan* (Table V) was highly homologous to ELIPs, which are thought to play a photoprotective role. ELIPs are known to bind to Chl (Adamska et al., 1999) and are expressed during processes involving both thylakoid assembly (Adamska et al., 1993) and disassembly (Adamska et al., 1992; Bartels et al., 1992; Adamska and Kloppstech, 1994; Bhalerao et al., 2003), including the chloroplast-to-chromoplast transition (Bruno and Wetzel, 2004). Their accumulation in the thylakoid also correlates closely with the production of ROS and light stress (Adamska et al., 1992, 1993; Adamska and Kloppstech, 1994; Hutin et al., 2003), in parallel with the reduced expression of Cab genes/proteins (Montané and Kloppstech, 2000; Kimura et al., 2003), as was observed in *nan* (Table III). In the *nan* mutant, a distinct time lag occurred between elevated levels of ELIP transcripts, which were seen at 190 DPA, long before color break or an equivalent increase in the wild type (Fig. 7), and increased levels of ELIP protein, which were not seen until color break and ripening (Fig. 5; Table V). However, a lack of correlation between changes in steady-state levels of ELIP transcripts and proteins was also noted in studies in Arabidopsis (Heddad et al., 2006). A recent report describing an *ELIP* gene knockout in Arabidopsis suggested that it did not affect tolerance to photoinhibition and photooxidative stress (Rossini et al., 2006), although the authors acknowledged that the many potential compensatory responses com-

plicates the interpretation of their data. Overall, a large body of evidence, including the coordinated up-regulation of ELIP mRNA and protein levels with those of a range of adaptations to oxidative stress, supports a role for ELIPs in protection against photooxidative damage.

In conclusion, the gene and protein expression profiling analyses and metabolite analyses reveal that the *nan* mutant shows numerous hallmarks of oxidative stress. Some of these are readily apparent, in the form of genes or proteins with a defined role in senescence or in providing protection against ROS (Table III). In other examples, no clear mechanistic relationship with a response to oxidative stress is apparent, even though there is precedence for an association based on previous microarray analyses, as is the case with β-amylase (Rossel et al., 2002; Table III). It is notable that *nan* shows substantial changes in gene and protein expression at the mature green stage, prior to the normal onset of Chl degradation or any detectable difference in Chl levels, compared with the wild type. This observation, together with the metabolite data, suggests that *nan* represents a new class of stay-green mutant with a lesion in a regulatory pathway that is upstream of *SGR* and that the mutant exhibits symptoms of oxidative stress prior to the onset of the normal degreening process.

MATERIALS AND METHODS

Plant Material and Ethylene Treatments

Fruits of *Citrus sinensis* 'Washington Navel' (wild type) and the *nan* stay-green mutant ('Navel Negra') were harvested from trees at the Instituto Valenciano de Investigaciones Agrarias and a commercial orchard, respectively. Sampling dates were July 26, 2004 (120 DPA), and then 180 (mature green stage), 190, 214, 224 (breaker stage), 248 (ripe stage), 260, and 275 DPA. For ethylene treatments, fruits were harvested at 180 DPA, when high levels of Chl were present in the flavedo, and treated with 10 μL L^{-1} ethylene at 20°C in a sealed chamber, and samples were taken at 0 and 72 h. Flavedo tissue from all samples was frozen in liquid nitrogen, powdered, and stored at −80°C until pigment analysis or RNA extractions. Aliquots of the frozen ground tissue were lyophilized prior to protein extraction.

Total Chl and Carotenoid Extraction and Quantification

Chls and carotenoids were extracted with methanol and chloroform as described by Rodrigo et al. (2003). Chl *a*, Chl *b*, and total Chl contents were calculated as described by Smith and Benítez (1955) after measuring the A_{644} and A_{662}. The pigment ethereal solution was then dried and saponified using 6% (w/v) KOH:methanol. Carotenoids were subsequently reextracted with diethyl ether until the hypophase was colorless. An aliquot of this extract was used for total carotenoid content quantification by measuring the A_{450} and using the extinction coefficient of β-carotene ($\varepsilon^{1\%} = 2{,}500$; Davies, 1976).

All steps were carried out on ice and under dim light to prevent photodegradation, isomerization, and structural changes in the carotenoids. At least three independent extractions were performed for each sample.

Chl and Derivative Extraction and HPLC Analysis

Chls and derivatives were extracted as described by Mínguez-Mosquera and Garrido-Fernández (1989), and Chls, Chl derivatives, and xanthophylls were retained in the dimethyl formamide phase and analyzed by HPLC. Chl *a* and *b* standards were purchased from Sigma. Chlorophyllide *a* was formed by enzymatic deesterification of Chl *a* (Mínguez-Mosquera et al., 1994). The C-13 epimer of Chl *a* was prepared by treatment with chloroform (Watanabe et al., 1984), and 13^2-OH-Chl *a* and *b* were obtained as described by Laitalainen et al. (1990). All standards were purified by normal-phase and reverse-phase TLC (Mínguez-Mosquera et al., 1991, 1993). The separation and quantification of Chl degradation products were carried out by HPLC (HP1100 Hewlett-Packard liquid chromatograph fitted with a HP1100 automatic injector) using a stainless-steel column (25 × 0.46 cm i.d.) packed with a 5-μm C_{18} Superior ODS-2 (Teknokroma). Separation was performed using an elution gradient (2 mL min^{-1}) with the mobile phases water:ion pair reagent:methanol (1:1:8, v/v/v) and methanol:acetone (1:1, v/v), as described by Mínguez-Mosquera et al. (1991). Sequential detection was performed with a photodiode array detector at 650 nm for series *b* and 666 nm for series *a* compounds. Data were collected and processed with an LC HP ChemStation (Rev.A.05.04). Pigments were identified by cochromatography with authentic samples and from their spectral characteristics. The on-line UV-visible spectra were recorded from 350 to 800 nm with the photodiode array detector. At least three independent extractions were performed for each sample.

CLH Activity

The method was an adaptation of that used by Terpstra and Lambers (1983). Flavedo tissue (5–10 g) was homogenized with 20 volumes of acetone at −20°C. The supernatant was removed by filtration, and the residue was treated again with 8 volumes of acetone. This operation was repeated until the supernatant was colorless. Finally, the precipitate was collected by vacuum filtration and left to dry at ambient temperature (20°C–25°C). From each 1 g of fruit, approximately 0.15 g of acetone powder was obtained. Extraction of the enzyme was carried out according to Johnson-Flanagan and Thiagarajah (1990). The acetone powder (0.5 g) was extracted with 15 mL of 5 mM sodium phosphate buffer (pH 7) containing 50 mM KCl and 0.24% (w/v) Triton X-100.

After centrifugation, the supernatant was used as a crude enzyme extract. The substrate, Chl *a*, was isolated from fresh spinach leaves by pigment extraction using acetone (Holden, 1976), followed by TLC separation as described by Mínguez-Mosquera and Garrido-Fernández (1989). The standard reaction mixture (1.1 mL) contained approximately 0.1 μmol of Chl *a* in acetone, 100 mM Tris buffer (pH 8.5) containing 0.24% (w/v) Triton-X-100, and enzyme extract in a 1:5:5 ratio. Chlorophyllide *a* levels were quantified as described by Mínguez-Mosquera et al. (1994), and the results are expressed as μmol h^{-1} g^{-1} fresh weight. At least three independent extractions were performed for each sample.

Ascorbic Acid Quantification

Discs of flavedo tissue were excised, frozen in liquid nitrogen, and ground to a fine powder, and 500 mg of each sample was homogenized in 5 mL of 2% metaphosphoric acid. After centrifugation (5,000*g*, 4°C, 10 min) and filtration, the ascorbic acid content of the supernatant was spectrophotometrically measured as described by Takahama and Oniki (1992) with a Cary 50 Bio spectrophotometer (Varian). Concentration was determined by monitoring the absorbance decrease at 265 nm due to the oxidation of ascorbate to deydroascorbate catalyzed by ascorbate oxidase (EC 1.10.3.3; from *Cucurbita* spp.). At least three independent determinations per sample were performed.

RNA Extraction and Real-Time RT-PCR

Total RNA was isolated from frozen flavedo using the RNeasy Plant Mini Kit (Qiagen) and treated with ribonuclease-free DNase (Qiagen) according to the manufacturer's instructions. UV light absorption spectrophotometry and agarose gel electrophoresis were performed to test RNA quality as described by Sambrook et al. (1989). Quantitative real-time RT-PCR was performed with a LightCycler 2.0 Instrument (Roche) equipped with LightCycler Software version 4.0 (Roche) as described by Alós et al. (2006). Specificity of the amplification reactions was assessed by postamplification dissociation curves and by sequencing the reaction products. To transform fluorescence intensity measurements into relative mRNA levels, a 10-fold dilution series of a RNA sample was used as a standard curve. Reproducible data were obtained after normalization to total RNA amounts accurately quantified with the RNA-specific fluorescent dye Ribogreen (Molecular Probes; Bustin, 2002; Hashimoto et al., 2004). Each sample was analyzed in triplicate and means ± SE were calculated. Induction values of 1-fold

were arbitrarily assigned to the 120-DPA sample for the natural ripening-associated gene expression. In the ethylene treatment experiment, the expression ratio between the treated and untreated fruits was calculated and log transformed. To validate the microarray data, real-time PCR of three selected genes was performed in triplicate and expression levels were log transformed. The sequences of the primers used for the real-time RT-PCR and associated references that were used for primer design are shown in Supplemental Table S2.

Genomic DNA Extraction and Real-Time PCR

Genomic DNA was isolated from frozen leaves using the DNeasy Plant Mini Kit (Qiagen) according to the manufacturer's instructions. UV light absorption spectrophotometry and agarose gel electrophoresis were performed to test DNA quality as described by Sambrook et al. (1989). DNA concentration was accurately quantified with the DNA-specific fluorescent dye Picogreen (Molecular Probes).

To determine the relative gene dosage of *SGR* in wild-type and *nan* fruits by quantitative real-time PCR, two specific oligonucleotide primers, sgrZCF (5′-AGTTTGGTTGCTGCTCTTGG-3′) and sgrZCR (5′-AGTGCGTTTTGCT GCTCATA-3′), were designed corresponding to positions 93 to 112 and 160 to 141, respectively, in the 566-bp *SGR* cDNA insert (accession no. CX308230). PCR was carried out with 1 ng of genomic DNA by adding 2 μL of LC FastStart DNA MasterPLUS SYBR Green I (Roche) and 2.5 pmol of each primer in a total volume of 10 μL. Incubations were carried out at 95°C for 10 min followed by 40 cycles at 95°C for 2 s, 55°C for 10 s, and 72°C for 15 s. Fluorescence intensity data were acquired during the 72°C extension step. Specificity of the amplification reactions was assessed by postamplification dissociation curves and by sequencing the reaction products. To transform fluorescence intensity measurements into relative DNA levels, a 10-fold dilution series of a DNA sample was used as a standard curve. Each sample was analyzed in triplicate and means ± SE were calculated.

Cloning and Sequencing the *SGR* Genomic Region

The promoter region of the citrus *SGR* gene was cloned from wild-type genomic DNA using the GenomeWalker Universal Kit (Clontech) following the manufacturer's instructions, except that six GenomeWalker libraries were constructed using the restriction enzymes *Dra*I, *Eco*RV, *Hin*cII, *Pvu*II, *Sca*I, and *Sma*I. Two gene-specific oligonucleotide primers, sgrA (5′-CTCTGACT-GAGTGGGAGAG-3′) and sgrB (5′-GTTGAAACGACCTGAC-3′), were designed corresponding to positions 66 to 48 and 31 to 16, respectively, in the 5′ end of the 566-bp *SGR* cDNA insert (accession no. CX308230). After two nested PCRs, a single 800-bp product was amplified from the *Dra*I library, cloned into the pCR2.1 vector (Invitrogen), and fully sequenced from both ends.

The genomic region containing the promoter and coding region of the *SGR* gene was cloned by PCR using genomic DNA from both *nan* and wild-type fruits using a forward primer specific for the 5′ end of the promoter region (sgrF, 5′-CTGACTCCCAGCGCAATTAC-3′) and a reverse primer specific for the 3′ end of the cDNA, adjacent to the poly(A) tail (sgrR, 5′-TCAAGATTCCATCTCAAAAGCTC-3′). The PCR mix consisted of 5 ng of genomic DNA, 1 μL of 10 mM dNTP mix, 5 pmol of each oligonucleotide, 2.5 μL of 10× reaction buffer, and 0.5 μL of Advantage 2 polymerase mix (Clontech). Touch-down PCR was carried out under the following conditions: 5 min at 95°C; 10 cycles of 30 s at 95°C, 1 min at the annealing temperature, decreasing by 1°C per cycle from 65°C to 55°C, and 3 min at 72°C; then 35 cycles of 30 s at 95°C, 1 min at 55°C, and 3 min at 72°C; and a final extension step at 72°C for 5 min. A single band of 1.2 kb was amplified from each of the genomic DNA samples. The products were cloned into the pCR2.1 vector, and plasmid DNA from 12 independent clones of each product was fully sequenced from both ends.

Microarray Hybridization and Analysis

Sample labeling, microarray hybridization and washing, and data acquisition and analysis were performed as described by Cercós et al. (2006). RNA was extracted from each sample with at least three biological replicates and independently processed, labeled, and hybridized to different microarrays. Differences in gene expression were considered to be significant when the P value was <0.001 and the induction or repression ratio was equal to or higher than 2-fold. Only high-quality PCR spots (Forment et al., 2005) were used for analyses.

2D-DIGE Analysis

Proteins were extracted from wild-type and *nan* flavedo tissue of mature green (180 DPA), breaker (224 DPA), and ripe (248 DPA) fruits as described by Saravanan and Rose (2004). Protein concentrations were quantified with the Bio-Rad protein assay using BSA as a standard. Protein labeling (50 μg per extract) was performed using Cy Dye DIGE fluors (Amersham Biosciences) according to the manufacturer's instructions. Immobilized pH gradient strips (24 cm, linear pH 4–7; Bio-Rad ReadyStrip; Bio-Rad) were rehydrated overnight with 450 μL of isoelectric focusing buffer containing the Cy Dye-labeled protein mixture described above and focused using a Protean IEF Cell (Bio-Rad) at 20°C. The following program was applied: a linear increase from 0 to 500 V over 1 h, 500 V to 10^4 V over 5 h, and then held at 10^4 V for a total of 100 kVh. After focusing, the proteins were reduced by incubating the immobilized pH gradient strips with 2% (w/v) dithiothreitol for 10 min and alkylated with 2% (w/v) iodoacetamide in 10 mL of equilibration buffer (6 M urea, 20% [v/v] glycerol, 3% [w/v] SDS, and 375 mM Tris-HCl, pH 8.8) for 10 min. The strips were then transferred to 12.5% SDS-PAGE gels for second-dimension electrophoresis with the Ettan Dalt six gel system (Amersham Biosciences) using SDS electrophoresis buffer (25 mM Tris, 192 mM Gly, and 0.1% [w/v] SDS) at 2 W per gel for 16 h. Four independent extracts were made from each sample, resulting in four replicate gels for each developmental stage. In each comparison, wild-type samples were labeled with the Cy3 dye in three gels and a dye swap was performed in the fourth.

Cy3 and Cy5 images were collected using a Typhoon scanner (Amersham Biosciences) in fluorescence mode at 100-μm resolution. Images were analyzed using ImageQuant version 5.2 (Amersham Biosciences) and Decyder version 4.0 (Amersham Biosciences). Spot volumes were determined after background subtraction and volume ratio values were normalized, so that the modal peak of volume ratios was zero. Differentially expressed spots were defined as those with a volume ratio above or below the 2 SD threshold. Final spot ratio values are means ± SE of four independent biological replicates for each developmental stage.

Protein Identification

Gels were fixed in water:methanol:acetic acid (83:10:7, v/v/v) for 2 h and subsequently stained with colloidal Coomassie Brilliant Blue G-250. Gel plugs containing protein spots of interest were manually excised, washed with 50 μL of water for 5 min and with 50 μL of acetonitrile and 50 mM ammonium bicarbonate (1:1, v/v) for 10 min, rehydrated in 15 μL of trypsin solution (10 ng μL^{-1} in 25 mM ammonium bicarbonate), and covered with 10 μL of 50 mM ammonium bicarbonate. After overnight incubation at 37°C, the supernatant was collected and peptides were reextracted sequentially with 60 μL of acetonitrile:formic acid (20:1, v/v) and 30 μL of acetonitrile:formic acid (180:1, v/v). The supernatants were combined and dried in a Speed-Vac (Thermo-Savant).

The samples were reconstituted in 10 μL of 0.1% formic acid and 2% acetonitrile (v/v) for liquid chromatography-electrospray ionization-tandem mass spectrometry analysis. The CapLC was carried out with an LC Packings Ultimate integrated capillary HPLC system equipped with a Switchos valve switching unit (Dionex). The gel-extracted peptides (6.4 μL) were injected using a Famous autosampler (Dionex) onto a C18 μ-precolumn cartridge (5 μm, 300 μm × 5 mm; Dionex) for on-line desalting and then separated on a PepMap C-18 RP capillary column (3 μm, 300 μm i.d. × 150 mm; Dionex). Peptides were eluted in a 30-min gradient of 5% to 45% acetonitrile in 0.1% formic acid at 4 $\mu L\ min^{-1}$. The CapLC was connected in-line to a hybrid triple-quadrupole linear ion trap mass spectrometer (4000 Q Trap; ABI/MDS Sciex) equipped with a Turbo V source. Data acquisition was performed using Analyst 1.4 software (Applied Biosystems) in the positive ion mode for information-dependent acquisition analysis. In information-dependent acquisition analysis, after each survey scan from m/z 400 to 1,600, an enhanced resolution scan was performed followed by tandem mass spectrometry (MS/MS) of the three highest intensity ions with multiple charge states. The MS/MS data were submitted to Mascot 1.9 for a database search against the NCBI nonredundant Green Plant database. The search was performed allowing one trypsin miscleavage site, and the peptide tolerance and MS/MS tolerance values were set to 0.8 and 2 D, respectively. Only significant scores defined by a Mascot

probability analysis (www.matrixscience.com/help/scoring_help.html#PBM) greater than "identity" were considered for assigning protein identity.

Immunoblot Analysis

Immunoblot analysis was carried with the same flavedo tissue samples used for the 2D-DIGE experiments. Ground flavedo tissue (500 mg) was resuspended in 2 mL of 50 mM Tris-HCl, pH 7.5, and 20 μL of 100 mM phenylmethylsulfonyl fluoride, incubated for 30 min at 2°C, and centrifuged at 10,000*g* at 4°C. The supernatant was collected and quantified by the Bradford assay (see above). Protein extracts (5 μg per lane) were separated by SDS-PAGE on 12.5% polyacrylamide gels (Bio-Rad). Gels were stained with SyproRuby (Bio-Rad) to confirm equivalent sample loading or transferred to Hybond ECL membranes, according to the manufacturer's instructions (Amersham Life Science). Immunoblot analysis was performed after blocking the membranes in 3% (w/v) bovine serum albumin and 0.02% (w/v) sodium azide in sterile phosphate-buffered saline (PBS)-Tween (1× PBS and 0.1% [v/v] Tween 20), using the ECL western-blotting kit, according to the manufacturer's instructions (Amersham Life Science). The blot was incubated with Rubisco antiserum (diluted 1:10,000 in PBS-Tween) followed by a 1:2,000 dilution of the horseradish peroxidase-conjugated secondary antibody. After each incubation with antiserum, the membrane was washed three times in PBS-Tween.

All of the microarray data described in this study were deposited in the ArrayExpress database (accession no. E-MEXP-967). The sequence data described in this study were deposited in GenBank (accession no. AM922109).

Supplemental Data

The following materials are available in the online version of this article.

Supplemental Figure S1. HPLC results of Chls and derivatives in wild-type and *nan* ripe fruit.

Supplemental Figure S2. Overlay images from 2D-DIGE analysis.

Supplemental Table S1. Microarray results for genes that showed statistically significant differences in expression levels between *nan* flavedo and Washington Navel wild-type flavedo at the mature green and ripe stages.

Supplemental Table S2. Oligonucleotides used as primers for real-time RT-PCR.

ACKNOWLEDGMENTS

We thank Isabel Sanchis, Israel Morte, and Angel Boix for technical support, and Tal Isaacson and Eric Schaffler for their help with two-dimensional gel analysis.

Received March 27, 2008; accepted May 5, 2008; published May 8, 2008.

LITERATURE CITED

Adamska I, Kloppstech K (1994) Low temperature increases the abundance of early light-inducible transcript under light stress conditions. J Biol Chem **269:** 30221–30226

Adamska I, Kloppstech K, Ohad I (1993) Early light-inducible protein in pea is stable during light stress but is degraded during recovery at low light intensity. J Biol Chem **268:** 5438–5444

Adamska I, Ohad I, Kloppstech K (1992) Synthesis of the early light-inducible protein is controlled by blue light and related to light stress. Proc Natl Acad Sci USA **89:** 2610–2613

Adamska I, Roobol-Bóza M, Lindahl M, Andersson B (1999) Isolation of pigment-binding early light-inducible proteins from pea. Eur J Biochem **260:** 453–460

Akhtar MS, Goldschmidt EE, John I, Rodoni S, Matile P, Grierson D (1999) Altered patterns of senescence and ripening in gf, a *stay-green* mutant of tomato (*Lycopersicon esculentum* Mill.). J Exp Bot **336:** 1115–1122

Alós E, Cercós M, Rodrigo MJ, Zacarías L, Talón M (2006) Regulation of color break in Citrus fruits: changes in pigment profiling and gene expression induced by gibberellins and nitrate, two ripening retardants. J Agric Food Chem **54:** 4888–4895

Apel K, Hirt H (2004) Reactive oxygen species: metabolism, oxidative stress and signal transduction. Annu Rev Plant Biol **55:** 373–399

Armstead I, Donnison I, Aubry S, Harper J, Hörtensteiner S, James C, Mani J, Moffet M, Ougham H, Roberts L, et al (2006) From crop to model to crop: identifying the genetic basis of the stay-green mutation in the *Lolium/Festuca* forage and amenity grasses. New Phytol **172:** 592–597

Armstead I, Donnison I, Aubry S, Harper J, Hörtensteiner S, James C, Mani J, Moffet M, Ougham H, Roberts L, et al (2007) Cross-species identification of Mendel's *I* locus. Science **315:** 73

Bachmann A, Fernández-López J, Ginsburg S, Thomas H, Bouwkamp JC, Solomos T, Matile P (1994) Stay-green genotypes of *Phaseolus vulgaris* L.: chloroplast proteins and chlorophyll catabolites during foliar senescence. New Phytol **126:** 593–600

Bain JM (1958) Morphological, anatomical and physiological changes in the developing fruit of the Valencia orange *Citrus sinensis* (L) Osbeck. Aust J Bot **6:** 1–24

Barber J, Andersson B (1992) Too much of a good thing: light can be bad for photosynthesis. Trends Biochem Sci **17:** 61–66

Barry CS, McQuinn RP, Chung MY, Besuden A, Giovannoni JJ (2008) Amino acid substitutions in homologs of the STAY-GREEN (SGR) protein are responsible for the *green-flesh* and *chlorophyll retainer* mutations of tomato and pepper. Plant Physiol **147:** 179–187

Bartels D, Hanke C, Schneider K, Michel D, Salamini F (1992) A desiccation-related ELIP-like gene from the resurrection plant *Craterostigma plantagineum* is regulated by light and ABA. EMBO J **11:** 2771–2778

Bhalerao R, Keskitalo J, Sterky F, Erlandsson R, Björkbacka H, Birve SJ, Karlsson J, Gardeström P, Gustafsson P, Lundeberg J, et al (2003) Gene expression in autumn leaves. Plant Physiol **131:** 430–442

Bouvier F, Backaus RA, Camara B (1998) Induction and control of chromoplast-specific carotenoid genes by oxidative stress. J Biol Chem **273:** 30651–30659

Bray EA (2002) Classification of genes differentially expressed during water-deficit stress in Arabidopsis: an analysis using microarray and differential expression data. Ann Bot (Lond) **89:** 803–811

Bruno AK, Wetzel CM (2004) The early light-inducible protein (ELIP) gene is expressed during chloroplast-to-chromoplast transition in ripening tomato fruit. J Exp Bot **408:** 2541–2548

Bustin SA (2002) Quantification of mRNA using real-time reverse transcription PCR (RT-PCR): trends and problems. J Mol Endocrinol **29:** 23–39

Cercós M, Soler G, Iglesias DJ, Gadea J, Forment J, Talón M (2006) Global analysis of gene expression during development and ripening of Citrus fruit flesh: a proposed mechanism for citric acid utilization. Plant Mol Biol **62:** 513–527

Cha KW, Lee YJ, Koh HJ, Lee BM, Nam YW, Paek NC (2002) Isolation, characterization, and mapping of the stay green mutant in rice. Theor Appl Genet **104:** 526–532

Chen F, D'Auria JC, Tholl D, Ross JR, Gershenzon J, Noel JP, Pichersky E (2003) An Arabidopsis gene for methylsalicylate biosynthesis, identified by a biochemical genomics approach, has a role in defense. Plant J **36:** 577–588

Cheung AY, McNellis T, Piekos B (1993) Maintenance of chloroplast components during chromoplast differentiation in the tomato mutant green flesh. Plant Physiol **101:** 1223–1229

Choe HC, Whang M (1986) Effects of ethephon on aging and photosynthetic activity in isolated chloroplasts. Plant Physiol **80:** 305–309

Davies BH (1976) Carotenoids. *In* TW Goodwin, ed, Chemistry and Biochemistry of Plant Pigments. Academic Press, New York, pp 38–165

Davies FS, Albrigo LG (1994) Citrus. CAB International, Oxon, UK, pp 202–215

Debnam PM, Fernie AR, Leisse A, Golding A, Bowsher CG, Grimshaw C, Knight JS, Emes MJ (2004) Altered activity of the P2 isoform of plastidic glucose 6-phosphate dehydrogenase in tobacco (*Nicotiana tabacum* cv. Samsun) causes changes in carbohydrate metabolism and response to oxidative stress in leaves. Plant J **38:** 49–59

de la Torre F, De Santis L, Suárez MF, Crespillo R, Cánovas FM (2006) Identification and functional analysis of a prokaryotic-type aspartate aminotransferase: implications for plant amino acid metabolism. Plant J **46:** 414–425

Efrati A, Eyal Y, Paran I (2005) Molecular mapping of the chlorophyll retainer (cl) mutation in pepper (*Capsicum* spp.) and screening for candidate genes using tomato ESTs homologous to structural genes of the chlorophyll catabolism pathway. Genome **48:** 347–351

Eilati SK, Budowski P, Monselise SP (1975) Carotenoid changes in the Shamouti orange peel during chloroplast-chromoplast transformation on and off the tree. J Exp Bot **26:** 624–632

Escoubas JM, Lomas M, Laroche J, Falkowski PG (1995) Light-intensity regulation of Cab gene transcription is signaled by the redox state of the plastoquinone pool. Proc Natl Acad Sci USA **92:** 10237–10241

Forment J, Gadea J, Huerta L, Abizanda L, Agustí J, Alamar S, Alós E, Andrés F, Arribas R, Beltrán JP, et al (2005) Development of a citrus genome-wide EST collection and cDNA microarray as resources for genomic studies. Plant Mol Biol **57:** 375–391

Fraser PD, Romer S, Shipton CA, Mills PB, Kiano JW, Misawa N, Drake RG, Schuch W, Bramley PM (2002) Evaluation of transgenic tomato plants expressing an additional phytoene synthase in a fruit-specific manner. Proc Natl Acad Sci USA **99:** 1092–1097

Fujita M, Fujita Y, Noutoshi Y, Takahashi F, Narusaka Y, Yamaguchi-Shinozaki K, Shinozaki K (2006) Crosstalk between abiotic and biotic stress responses: a current view from the points of convergence in the stress signaling networks. Curr Opin Plant Biol **9:** 436–442

Gadjev I, Vanderauwera S, Gechev TS, Laloi C, Minkov IN, Shulaev V, Apel K, Inzé D, Mittler R, Van Breusegem F (2006) Transcriptomic footprints disclose specificity of reactive oxygen species signaling in Arabidopsis. Plant Physiol **141:** 436–445

Gan S, Amasino RM (1995) Inhibition of leaf senescence by autoregulated production of cytokinin. Science **270:** 1986–1988

García-Luis A, Fornes F, Guardiola JL (1986) Effects of gibberellin A_3 and cytokinins on natural post-harvest, ethylene-induced pigmentation of Satsuma mandarin peel. Physiol Plant **68:** 271–274

Gepstein S, Sabehi G, Carp MJ, Hajouj T, Nesher MFO, Yariv I, Dor C, Bassani M (2003) Large-scale identification of leaf senescence-associated genes. Plant J **36:** 629–642

Guiamét JJ, Giannibelli MC (1994) Inhibition of the degradation of chloroplast membranes during senescence in nuclear 'stay green' mutants of soybean. Physiol Plant **91:** 395–402

Guiamét JJ, Giannibelli MC (1996) Nuclear and cytoplasmic 'stay-green' mutations of soybean alter the loss of leaf soluble proteins during senescence. Physiol Plant **96:** 655–661

Guo Y, Cai Z, Gan S (2004) Transcriptome of Arabidopsis leaf senescence. Plant Cell Environ **27:** 521–549

Harpaz-Saad S, Azoulay T, Arazi T, Ben-Yaakov E, Mett A, Shiboleth YM, Hörtensteiner S, Gidoni D, Gal-On A, Goldschmidt EE, et al (2007) Chlorophyllase is a rate-limiting enzyme in chlorophyll catabolism and is posttranslationally regulated. Plant Cell **19:** 1007–1022

Hashimoto JG, Beadles-Bohling AS, Wiren KM (2004) Comparison of RiboGreen and 18S rRNA quantitation for normalizing real-time RT-PCR expression analysis. Biotechniques **36:** 54–60

Heddad M, Adamska I (2000) Light stress-regulated two-helix proteins in Arabidopsis related to the chlorophyll a/b binding gene family. Proc Natl Acad Sci USA **97:** 3741–3746

Heddad M, Norén H, Reisewr V, Dunaeva M, Andersson B, Adamska I (2006) Differential expression and localization of early light-induced proteins in Arabidopsis. Plant Physiol **142:** 75–87

Hendry GAF, Houghton JD, Brown SB (1987) The degradation of chlorophyll: a biological enigma. New Phytol **107:** 255–302

Holden M (1976) Analytical methods chlorophylls. *In* TW Goodwin, ed, Chemistry and Biochemistry of Plant Pigments, Vol II. Academic Press, London, pp 1–37

Hörtensteiner S (2006) Chlorophyll degradation during senescence. Annu Rev Plant Biol **57:** 55–77

Hutin C, Nussaume L, Moise N, Moya I, Kloppstech K, Havaux M (2003) Early light-induced proteins protect Arabidopsis from photooxidative stress. Proc Natl Acad Sci USA **100:** 4921–4926

Iglesias DJ, Calatayud A, Barreno E, Primo-Millo E, Talon M (2006) Responses of citrus plants to ozone: leaf biochemistry, antioxidant mechanisms and lipid peroxidation. Plant Physiol Biochem **44:** 125–131

Iglesias DJ, Tadeo FR, Legaz F, Primo-Millo E, Talon M (2001) In vivo sucrose stimulation of colour change in citrus fruits epicarps: interactions between nutritional and hormonal signals. Physiol Plant **112:** 244–250

Inada S, Ohgishi M, Mayama T, Okada K, Sakai T (2004) RPT2 is a signal transducer involved in phototropic response and stomatal opening by association with phototropin 1 in *Arabidopsis*. Plant Cell **16:** 887–896

Jacob-Wilk D, Holland D, Goldschmidt EE, Riov J, Eyal Y (1999) Chlorophyll breakdown by chlorophyllase: isolation and functional expression of the Chlase1 gene from ethylene-treated Citrus fruit and its regulation during development. Plant J **20:** 653–661

Jiang H, Li M, Ling N, Yan H, Xu X, Liu J, Xu Z, Chen F, Wu G (2007) Molecular cloning and function analysis of the *stay green* gene in rice. Plant J **52:** 197–209

John I, Drake R, Farrell A, Cooper W, Lee P, Horton P, Grierson D (1995) Delayed leaf senescence in ethylene deficient ACC-oxidase antisense tomato plants: molecular and physiological analysis. Plant J **7:** 483–490

Johnson-Flanagan A, Thiagarajah M (1990) Degreening in canola (*Brassica napus*, cv Westar) embryos under optimum conditions. J Plant Physiol **136:** 180–186

Jordan BR (2002) Molecular responses of plant cells to UV-B stress. Funct Plant Biol **29:** 909–916

Kao CH, Yang SF (1983) Role of ethylene in the senescence of detached rice leaves. Plant Physiol **73:** 881–885

Kato M, Ikoma Y, Matsumoto H, Sugiura M, Hyodo H, Yano M (2004) Accumulation of carotenoids and expression of the carotenoid biosynthetic genes during maturation in citrus fruit. Plant Physiol **134:** 1–14

Kim HS, Yu Y, Snesrud EC, Moy LP, Linford LD, Haas BJ, Nierman WC, Quackenbush J (2005) Transcriptional divergence of the duplicated oxidative stress-responsive genes in the Arabidopsis genome. Plant J **41:** 212–220

Kimura M, Yamamoto YY, Seki M, Sakurai T, Sato M, Abe T, Yoshida S, Manabe K, Shinozaki K, Matsui M (2003) Identification of Arabidopsis genes regulated by high light-stress using cDNA microarray. Photochem Photobiol **77:** 226–233

Kuehn GD, Phillips GC (2005) Role of polyamines in apoptosis and other recent advances in plant polyamines. CRC Crit Rev Plant Sci **24:** 123–130

Kusaba M, Ito H, Morita R, Iida S, Sato Y, Fujimoto M, Kawasaki S, Tanaka R, Hirochika H, Nishimura M, et al (2007) Rice NON-YELLOW COLORING1 is involved in light-harvesting complex II and grana degradation during leaf senescence. Plant Cell **19:** 1362–1375

Laitalainen T, Pitkänen J, Hynninen P (1990) Diastereoselective 13^2-hydroxylation of chlorophyll a with SeO_2. *In* Abstracts of the 8th International IUPAC Conference on Organic Synthesis. IUPAC, Helsinki, p 246

Lam H-M, Hsieh M-H, Coruzzi G (1998) Reciprocal regulation of distinct asparagine synthetase genes by light and metabolites in Arabidopsis. Plant J **16:** 345–353

Lee GJ, Roseman AM, Saibil HR, Vierling E (1997) A small heat shock protein stably binds heat-denatured model substrates and can maintain a substrate in a folding-competent state. EMBO J **16:** 659–671

Li XP, Gan R, Li PL, Ma YY, Zhang LW, Zhang R, Wang Y, Wang NN (2006) Identification and functional characterization of a leucine-rich repeat receptor-like kinase gene that is involved in regulation of soybean leaf senescence. Plant Mol Biol **61:** 829–844

Luquez VM, Guiamét JJ (2002) The stay green mutations d1 and d2 increase water stress susceptibility in soybeans. J Exp Bot **376:** 1421–1428

Mahalingam R, Shah N, Scrymgeour A, Fedoroff N (2005) Temporal evolution of the Arabidopsis oxidative stress response. Plant Mol Biol **57:** 709–730

Mínguez-Mosquera MI, Gallardo-Guerrero L, Gandul-Rojas B (1993) Characterization and separation of oxidized derivatives of pheophorbide a and b by thin-layer and high-performance liquid chromatography. J Chromatogr **633:** 295–299

Mínguez-Mosquera MI, Gandul-Rojas B, Gallardo-Guerrero L (1994) Measurement of chlorophyllase activity in olive fruit (*Olea europaea*). J Biochem **116:** 263–268

Mínguez-Mosquera MI, Gandul-Rojas B, Montaño-Asquerino A, Garrido-Fernández J (1991) Determination of chlorophylls and carotenoids by HPLC during olive lactic fermentation. J Chromatogr **585:** 259–266

Mínguez-Mosquera MI, Garrido-Fernández J (1989) Chlorophyll and carotenoid presence in olive fruit (*Olea europaea* L.). J Agric Food Chem **37:** 1–7

Mitler R, Vanderauwera S, Gollery M, Breusegem FV (2004) Reactive oxygen gene network of plants. Trends Plant Sci **9:** 490–498

Montané MH, Kloppstech K (2000) The family of light-harvesting-related proteins (LHCs, ELIPs, HLIPs): was the harvesting of life their primary function? Gene **258:** 1–8

Neta-Sharir I, Isaacson T, Lurie S, Weiss D (2005) Dual role for tomato heat shock protein 21: protecting photosystem II from oxidative stress and promoting color changes during fruit maturation. Plant Cell **17:** 1829–1838

Niyogi KK (1999) Photoprotection revisited. Annu Rev Plant Physiol Plant Mol Biol **50:** 333–359

Oh MH, Kim JH, Moon YH, Lee CH (2004) Defects in a proteolytic step of light-harvesting complex II in an Arabidopsis stay-green mutant, *ore10*, during dark-induced leaf senescence. J Plant Biol **47:** 330–337

Oh MH, Moon YH, Lee CH (2003) Increased stability of LHCII by aggregate formation during dark-induced leaf senescence in the Arabidopsis mutant, *ore 10.* Plant Cell Physiol **44:** 1368–1377

Park SY, Yu JW, Park JS, Li J, Yoo SC, Lee NY, Lee SK, Jeong SW, Seo HS, Koh HJ, et al (2007) The senescence-induced staygreen protein regulates chlorophyll degradation. Plant Cell **19:** 1649–1664

Rampino P, Spano G, Pataleo S, Mita G, Napier JA, Di Fonzo N, Shewry PR, Perrotta C (2006) Molecular analysis of a durum wheat 'stay green' mutant: expression pattern of photosynthesis-related genes. J Cereal Sci **43:** 160–168

Ren G, An K, Liao Y, Zhou X, Cao Y, Zhao H, Ge X, Kuai B (2007) Identification of a novel chloroplast protein AtNYE1 regulating chlorophyll degradation during leaf senescence in Arabidopsis. Plant Physiol **144:** 1429–1441

Rizhsky L, Davletova S, Liang H, Mittler R (2004) The zinc-finger protein Zat12 is required for cytosolic ascorbate peroxidase 1 expression during oxidative stress in Arabidopsis. J Biol Chem **279:** 11736–11743

Roca M, James J, Pruzinska A, Hortensteiner S, Thomas H, Ougham H (2004) Analysis of the chlorophyll catabolism pathway in leaves of an introgression senescence mutant of *Lolium temulentum.* Phytochemistry **65:** 1231–1238

Roca M, Mínguez-Mosquera MI (2006) Chlorophyll catabolism pathway in fruits of *Capsicum annuum* (L.): stay-green versus red fruits. J Agric Food Chem **54:** 4035–40

Rodrigo MJ, Marcos J, Alférez F, Mallent MD, Zacarías L (2003) Characterization of Pinalate, a novel *Citrus sinensis* mutant with a fruit-specific alteration that results in yellow pigmentation and decreased ABA content. J Exp Bot **54:** 727–738

Rodrigo MJ, Marcos JF, Zacarías L (2004) Biochemical and molecular analysis of carotenoid biosynthesis in flavedo of orange (*Citrus sinensis* L.) during fruit development and maturation. J Agric Food Chem **52:** 6724–6731

Ronning CM, Bouwkamp JC, Solomos T (1991) Observations on the senescence of a mutant non-yellowing genotype of *Phaseolus vulgaris* L. J Exp Bot **235:** 235–241

Rose JKC, Bashir S, Giovannoni JJ, Jahn MM, Saravanan RS (2004) Tackling the plant proteome: practical approaches, hurdles and experimental tools. Plant J **39:** 715–733

Rossel JB, Wilson IW, Pogson BJ (2002) Global changes in gene expression in response to high light in Arabidopsis. Plant Physiol **130:** 1109–1120

Rossini S, Casazza AP, Engelmann EC, Havaux M, Jennings RC, Soave C (2006) Suppression of both ELIP1 and ELIP2 in Arabidopsis does not affect tolerance to photoinhibition and photooxidative stress. Plant Physiol **141:** 1264–1273

Sambrook J, Fitsch EF, Maniatis T (1989) Molecular Cloning: A Laboratory Manual. Cold Spring Harbor Laboratory Press, Cold Spring Harbor, NY

Saravanan RS, Rose JKC (2004) A critical evaluation of sample extraction techniques for enhanced proteomic analysis of recalcitrant plant tissues. Proteomics **4:** 2522–2532

Sato Y, Morita R, Nishimura M, Yamaguchi H, Kusaba M (2007) Mendel's green cotyledon gene encodes a positive regulator of the chlorophyll-degrading pathway. Proc Natl Acad Sci USA **104:** 14169–14174

Smart CM, Scofield SR, Bevan MW, Dyer TA (1991) Delayed leaf senescence in tobacco plants transformed with *tmr*, a gene for cytokinin production in *Agrobacterium.* Plant Cell **3:** 647–656

Smith JHC, Benítez A (1955) Chlorophylls. *In* K Paech, MM Tracey, eds, Modern Methods of Plant Analysis. Springer, Berlin, pp 142–196

Spano G, Di Fonzo N, Perrotta C, Platani C, Ronga G, Lawlor DW, Napier JA, Shewry PR (2003) Physiological characterisation of 'stay green' mutants in durum wheat. J Exp Bot **386:** 1415–1420

Sun W, van Montagu M, Verbruggen N (2002) Small heat shock proteins and stress tolerance in plants. Biochim Biophys Acta **1577:** 1–9

Takahama U, Oniki T (1992) Regulation of peroxidase-dependent oxidation of phenolics in the apoplast of spinach leaves by ascorbate. Plant Cell Physiol **33:** 379–387

Tanaka R, Oster U, Kruse E, Rudiger W, Grimm B (1999) Reduced activity of geranylgeranyl reductase leads to loss of chlorophyll and tocopherol and to partially geranylgeranylated chlorophyll in transgenic tobacco plants expressing antisense RNA for geranylgeranyl reductase. Plant Physiol **120:** 695–704

Terpstra W, Lambers J (1983) Interactions between chlorophyllase, chlorophyll a, plants lipids and Mg^{2+}. Biochim Biophys Acta **746:** 23–31

Thomas H (1987) *Sid*: a Mendelian locus controlling thylakoid membrane disassembly in senescing leaves of *Festuca pratensis.* Theor Appl Genet **73:** 551–555

Thomas H, Howarth CJ (2000) Five ways to stay green. J Exp Bot **51:** 329–337

Thomas H, Ougham H, Canter P, Donnison I (2002) What stay-green mutants tell us about nitrogen remobilization in leaf senescence. J Exp Bot **53:** 801–808

Thomas H, Schellenberg M, Vicentini F, Matile P (1996) Gregor Mendel's green and yellow pea seeds. Bot Acta **109:** 3–4

Tosti N, Pasqualini S, Borgogni A, Ederli L, Falistocco E, Crispi S, Paolocci F (2006) Gene expression profiles of O_3-treated Arabidopsis plants. Plant Cell Environ **29:** 1686–1702

Trebitsh T, Goldschmidt EE, Riov J (1993) Ethylene induces de novo synthesis of chlorophyllase, a chlorophyll degrading enzyme, in Citrus fruit peel. Proc Natl Acad Sci USA **90:** 9441–9445

Vicentini F, Hörtensteiner S, Schellenberg M, Thomas H, Matile P (1995) Chlorophyll breakdown in senescent leaves: identification of the biochemical lesion in a stay-green genotype of *Festuca pratensis* Huds. New Phytol **129:** 247–252

Watanabe T, Hongu A, Honda K, Nakazato M, Konno M, Saithoh S (1984) Preparation of chlorophylls and pheophytins by isocratic liquid chromatography. Anal Chem **56:** 251–256

Wong CE, Li Y, Labbe A, Guevara D, Nuin P, Whitty B, Diaz C, Golding GB, Gray GR, Weretilnyk EA, et al (2006) Transcriptional profiling implicates novel interactions between abiotic stress and hormonal responses in Thellungiella, a close relative of Arabidopsis. Plant Physiol **140:** 1437–1450

Woo HR, Chung KM, Park JH, Oh SA, Ahn T, Hong SH, Jang SK, Nam HG (2001) ORE9, an F-box protein that regulates leaf senescence in *Arabidopsis.* Plant Cell **13:** 1779–1790

Yamamoto A, Bhuiyan NMH, Watidee R, Tanaka Y, Esaka M, Oba K, Jagendorf AT, Takabe T (2005) Suppressed expression of the apoplastic ascorbate oxidase gene increases salt tolerance in tobacco and Arabidopsis plants. J Exp Bot **56:** 1785–1796

Young R, Jahn O (1972) Ethylene-induced carotenoid accumulation in citrus fruit rinds. J Am Soc Hortic Sci **97:** 258–261

Zhao J, Williams CC, Last RL (1998) Induction of *Arabidopsis* tryptophan pathway enzymes and camalexin by amino acid starvation, oxidative stress, and an abiotic elicitor. Plant Cell **10:** 359–370